International Journal of Multiphase Flow 114 (2019) 66–81

Contents lists available at ScienceDirect

International Journal of Multiphase Flow

journal homepage: www.elsevier.com/locate/ijmulflow

Experimental observations of bubbling regimes at in-line multi-orifice bubblers

Antonio Capponi*, Edward W. Llewellin

Department of Earth Sciences, Durham University, Durham, UK, DH1 3LE

ARTICLE INFO

Article history:
Received 22 October 2018
Revised 10 January 2019
Accepted 21 February 2019
Available online 22 February 2019

Keywords:
Bubble formation
Gas sparger
Submerged orifices
Multi-orifice
Bubble period
Bubble formation time

ABSTRACT

Bubble formation and bubbling regimes are well-characterized for the cases of single-orifice bubblers and industrial perforated plates. However, bubbling regimes from bubblers with multiple in-line orifices remain poorly described. Here, we investigate the dynamics of bubble formation at both single-orifice and multi-orifice bubblers, with one, three, five and nine in-line orifices in an 80-cm-long bubbler. We use high-speed videography and image processing to identify the effects of bubbler volume, and the number, spacing, and diameter of orifices, on bubbling regimes, bubble period, and bubble formation time. We identify five main bubbling regimes based on synchronization among orifices, and discuss the parameters affecting the bubbling dynamics. Decreasing bubbler volume leads to a decrease in bubble volume and bubble period, and enhances synchronization. Increasing orifice diameter leads to an increase in bubble volume and enhances synchronization. Spacing between orifices doesn't play an important role in determining the bubbling regime. Based on the experimental observations, we develop new bubbling regime maps constructed using the dimensionless Capacitance number and Weber number.

1. Introduction

Bubble formation plays an important role in many industrial and environmental settings, such as cooling systems, gas absorption units, air-lift reactors, metallurgic processing, and waste-water treatment. Consequently, a large body of industrial literature exists on the processes associated with bubble formation – usually generated via a gas chamber fitted with orifices or nozzles – and the subsequent dispersion of the bubbles into the liquid phase (e.g., Leibson et al., 1956; Davidson and Schueler, 1960a, b; Kumar and Kuloor, 1970; Jamialahmadi et al., 2001; Badam et al., 2007).

Previous experimental investigations have identified three different conditions under which bubbles may form at an orifice: constant-flow conditions, where gas flux from the chamber to the forming bubble is constant; constant-pressure conditions, where pressure in the chamber is constant; and intermediate conditions, where both flux into the forming bubble and the chamber pressure vary (e.g., Davidson and Schueler, 1960a, b; Kumar and Kuloor, 1970; Tsuge and Hibino, 1983). Since this classification was proposed, most of the experimental studies have considered bubble formation at a single orifice under either constant-flow conditions (e.g., Jamialahmadi et al., 2001; Buwa et al., 2007) or constant-pressure conditions (e.g., Davidson and Schueler, 1960a, b; Satyanarayan et al., 1969), and a number of different bubbling regimes have been identified. At low gas flow rates, bubbles can form singly and periodically, without interacting with one another. Increasing gas flow rates leads to bubble interaction, and processes of pairing, coalescence and chaining (e.g., Muller and Prince, 1972; Wang et al., 2017). Various studies have shown that bubble volume, velocity, and bubbling regimes for differing gas flow rates are influenced by properties of the gas phase (e.g., Kumar and Kuloor, 1970; Idogawa, 1987), liquid rheology (e.g., Kumar and Kuloor, 1970; Clift et al., 1978; Jamialahmadi et al., 2001), chamber volume (e.g., Kumar and Kuloor, 1970; Tsuge and Hibino, 1983) and orifice diameter (e.g., Badam et al., 2007; Di Bari and Robinson, 2013). Higher gas density accelerates the detachment time of a bubble for large diameter orifices, while for very small diameters the gas density has negligible effects on the detachment time (e.g., Kumar and Kuloor, 1970; Kulkarni and Joshi, 2005). The influence of liquid viscosity on bubble size depends on the gas flow rate: for low flow rates, the bubble volume is independent of viscosity, while for high flow rates, bubble volume increases with an increase in liquid viscosity (e.g., Jamialahmadi et al., 2001). Variations in the chamber volume, together with changes in orifice diameter, dictate bubble volume and frequency; an increase in either of these parameters leads to a bigger bubble volume and increase in frequency (e.g., Kumar and Kuloor, 1970; Clift et al., 1978;

* Corresponding author.
E-mail address: antonio.capponi@durham.ac.uk (A. Capponi).

https://doi.org/10.1016/j.ijmultiphaseflow.2019.02.008

Tsuge and Hibino, 1983; Badam et al., 2007; Di Bari and Robinson, 2013).

Work on bubbling through a single orifice has focused on bubble formation at relatively low flow rates; typically, the highest flow rate used is between 0.5 and 3 l/min (e.g., Davidson and Schueler, 1960a, b; Jamialahmadi et al., 2001; Nahra and Kamotani, 2003; Badam et al., 2007). Investigation of bubblers with multiple orifices has focussed mainly on spargers, or industrial perforated plates, with many closely-spaced orifices (such as sieve-plate spargers). Investigation of bubblers with multiple discrete orifices fed from a common gas chamber has been restricted to two orifices (e.g., Xie and Tan, 2003) or up to thirteen orifices arranged in different geometrical patterns (e.g., Ruzicka et al., 1999, 2000). Results show that bubbling may be synchronous or asynchronous, with transitional modes in between in which – depending on the flow rate – only some of the open orifices are active, or bubble formation from some orifices becomes asynchronous (Ruzicka et al., 1999; Xie and Tan, 2003). The degree of synchronization is greater for orifices that are further apart (Ruzicka et al., 2000). For multi-orifice bubblers, the importance of the volume of the gas chamber in determining bubble volume and frequency diminishes as the number of active orifices increases (e.g., Ruzicka et al., 1999; Xie and Tan, 2003; Kulkarni and Joshi, 2005).

Notwithstanding these studies, bubble formation in a multi-orifice system remains under-investigated, particularly for linear bubblers – to our knowledge, no study has investigated the behaviour of linear bubblers with more than four in-line, discrete orifices. The effects on bubbling regime of parameters such as gas flow rate, and diameter, number, and spacing of orifices, are relatively unexplored. The lack of experimental data on this subject, compared to single-orifice bubblers, has prevented the development of models of bubbling at multiple orifices (Kulkarni and Joshi, 2005). Here, we aim to address this gap by providing experimental details on the bubbling modes from linear bubblers. First, we investigate the bubbling dynamics from a single-orifice, to connect our work to existing literature observations, and extend them to higher gas flow rates. Then, we move to multi-orifice systems, describing and quantifying bubbling regimes, and the effects of changing gas flow rate, orifice diameter, and bubbler volume, on bubble formation time, bubble period, and transitions in bubbling modes.

2. Experimental set-up and scaling

We performed experiments using the apparatus shown in Fig. 1, which consists of a large glass tank, a stainless steel bubbler (1), and a gas injection system (2–4). The glass tank has dimensions $1 \times 0.5 \times 0.5$ m (length, breadth, height) and is open to the atmosphere. The tank was filled to a depth of 40 cm with water (viscosity $\mu = 0.001$ Pa s, density $\rho = 1000$ kg/m^3, surface tension $\sigma = 0.07$ N m^{-1}). Compressed air was introduced into the bubbler from both ends, using two flexible hoses of equal length. To avoid pressure fluctuations, the air from the compressor was first passed through a pressure regulator (3), and then through a gas flow meter (2; flow range 0.2–10 l/min) with an integrated needle valve to allow precise adjustment of the flow.

The bubblers were constructed using stainless steel pipes with wall thickness 1.5 mm, with three different internal diameters ($D_b = 0.7$, 1.5, and 2.5 cm) to give three different bubbler volumes ($V_b = 3.1 \times 10^{-5}$, 6.3×10^{-5}, and 4.0×10^{-4} m^3). The bubblers were supported by two aluminium tracks and held in place by lead blocks, so that the orifices were 7.5 cm above the bottom of the tank. Rows of 9 orifices of diameter $D_0 = 1$, 2, and 3 mm were carefully drilled in line. During experiments, we used sealing fasteners to close some of the orifices, to have different configurations of N orifices with spacing S (Fig. 1). In any single experiment, only orifices of the same diameter were open. The volumetric gas flow rate, Q, was varied in the range 0.2–10 l/min, thus covering low gas flow rates already investigated in the literature, as well as higher flow rates that have not previously been reported. The entire experimental suite comprises 944 individual experiments; across the suite, the parameters V_b, D_b, Q, D_0, N, and S (Table 1) were varied independently and systematically. All experiments were imaged with a high-speed camera, at 330 frames per second.

Table 1
Summary of experimental parameters.

Quantity	Symbol	Units	Values
Bubbler volume	V_b	m^3	3.1×10^{-5}, 6.3×10^{-5}, 4.0×10^{-4}
Bubbler diameter	D_b	m	0.007, 0.01, 0.025
Gas flow rate	Q	l/min	0.2, 0.5, 0.8, 1.1, 2, 3.5, 5, 10
Orifice diameter	D_0	m	0.001, 0.002, 0.003
Number of orifices	N	–	1, 3, 5, 9
Orifice spacing	S	m	0.035, 0.075, 0.15
Orifice configuration	–	–	See Fig. 1
Liquid depth	h	m	0.40

Variations in bubbler volume and number of orifices were captured using the dimensionless Capacitance number (Tsuge and Hibino, 1983):

$$N_c = \frac{4V_b \gamma g(\rho_l - \rho_g)}{N\pi D_o^2 \rho_g c^2} \tag{1}$$

where γ is the gas specific heat ratio, g is gravitational acceleration, ρ_l and ρ_g the density of the liquid and the gas respectively, and c the sound speed in the gas. The Capacitance number has previously been shown to discriminate bubbling regimes (e.g., Kumar and Kuloor, 1970; Tsuge and Hibino, 1983): for constant-flow conditions $N_c < 1$; for intermediate conditions $1 < N_c < 9$; and for constant-pressure conditions $N_c > 9$. For the selected bubbler volumes and orifice diameters, the Capacitance number for our experiments spans the range $0.05 < N_c < 50$; we thus cover all three regimes (Fig. 2).

Two additional dimensionless parameters are relevant: the Eötvös number (or Bond number):

$$\mathrm{Eo} = \frac{\rho_l g D_0^2}{\sigma}, \tag{2}$$

which describes the balance of buoyancy and surface tension stresses, and the Froude number:

$$\mathrm{Fr} = \frac{V_g}{\sqrt{gD_o}}, \tag{3}$$

which is a dimensionless velocity, in which V_g is the average gas velocity at each orifice, given by dividing Q by the total area of the orifices:

$$V_g = \frac{Q}{N\pi\left(\frac{D_0}{2}\right)^2}. \tag{4}$$

Combining Eo and Fr, we obtain the dimensionless Weber number We, expressed as a function of the orifice diameter (e.g., Tsuge and Hibino, 1983):

$$\mathrm{We} = \mathrm{EoFr}^2 = \frac{\rho_l D_o V_g^2}{\sigma}. \tag{5}$$

2.1. Data analysis

We performed image analysis using Fiji, an open source image processing package built on ImageJ (Schindelin et al., 2012). Videos of the experiments were used to calculate bubble period, formation time, and average bubble diameters and volumes. We defined

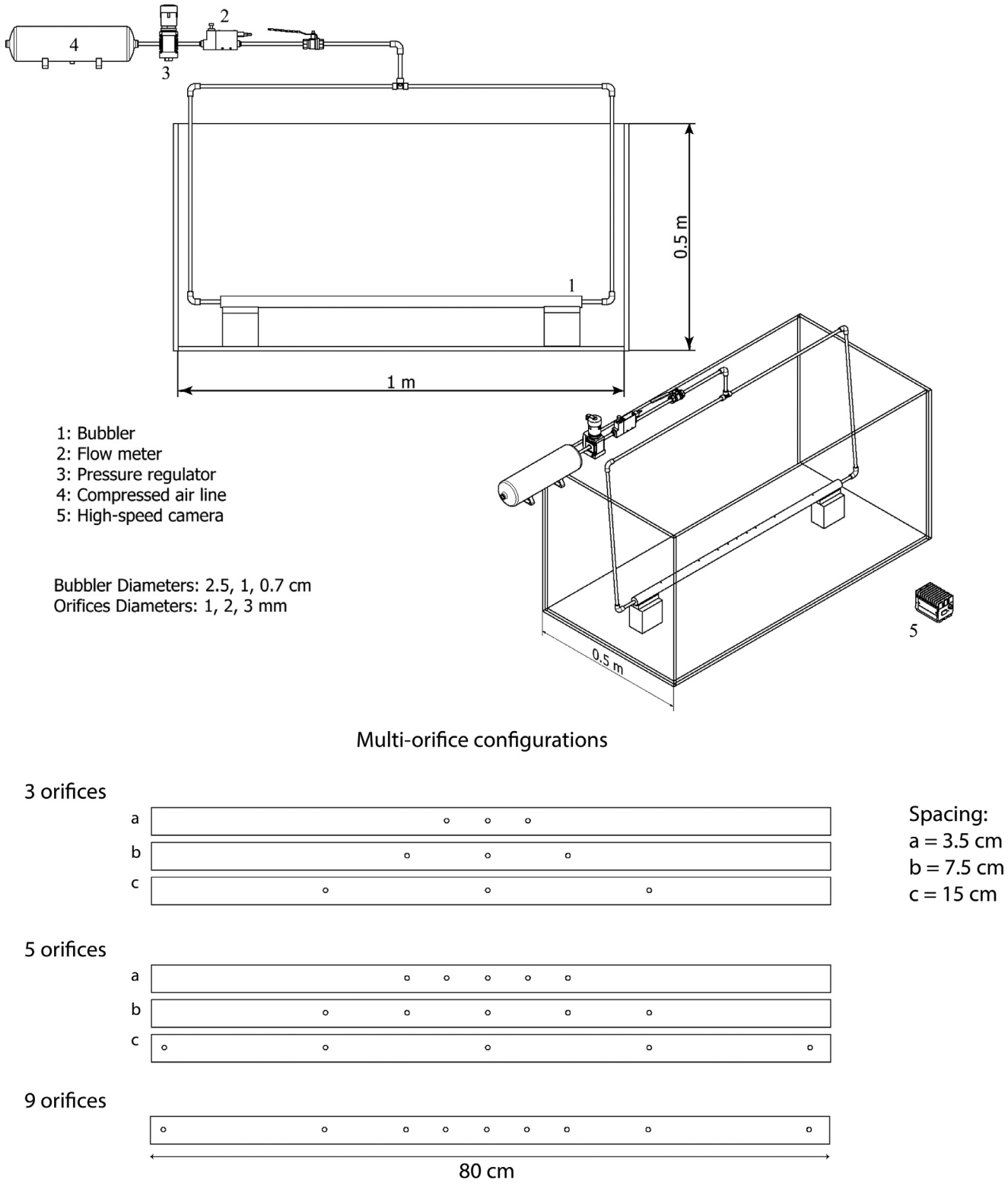

Fig. 1. Experimental set-up (main glass tank; 1. stainless steel bubbler; 2. gas flow meter; 3. pressure regulator; 4. compressed air line; 5. high-speed camera system) and configurations of orifices used.

the spatial scale for the videos using a calibration image for each experiment so that Fiji automatically converted any pixel distance to centimetres.

The duration and timing of bubble formation was extracted from the videos as follows. First, each image in the video was converted from RGB color to 8-bit grayscale. Flickering in light intensity was corrected by applying the 'Bleach Correction' in Fiji, using the 'Histogram Matching' method. This method calculates the pixel grayscale histogram for the first frame, and then adjusts the histograms for all the successive frames to match the first. From the flicker-free stack, we isolated the bubbles by first subtracting the background from the stack so that only the bubbles are visible, then we created binary images by applying a threshold to the stack (Fig. 3). First, we applied an automatic threshold to the stack. Then,

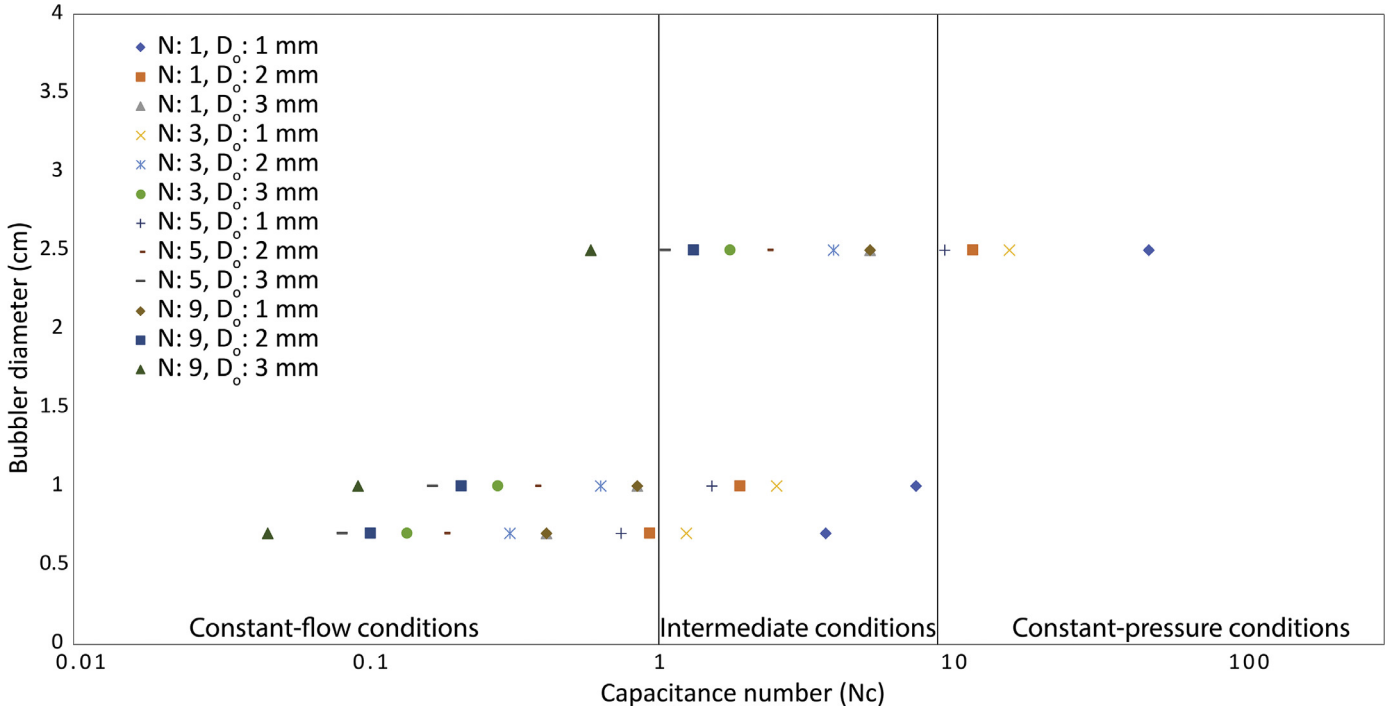

Fig. 2. Variations of flow conditions in which bubbles form depending on number (N) and diameter (D_O) of open orifices (symbols), as a function of the dimensionless Capacitance number, N_c, for all bubbler diameters used (cm). For $N_c < 1$: constant-flow conditions; $1 < N_c < 9$: intermediate conditions; $N_c > 9$: constant-pressure conditions.

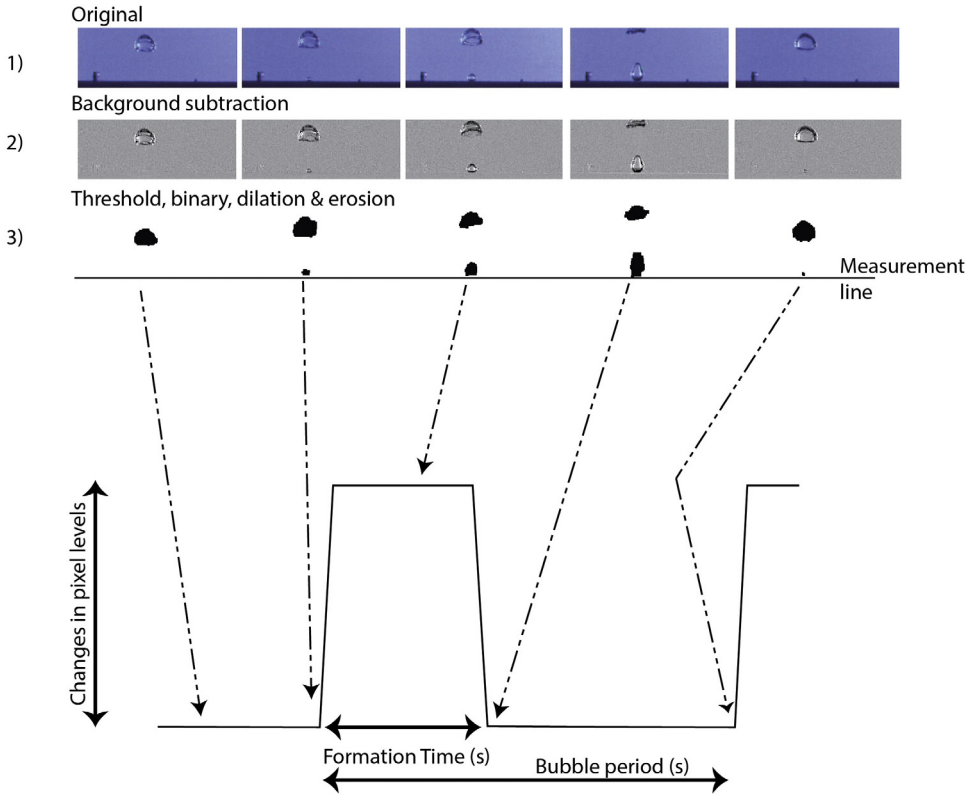

Fig. 3. Sequence of image processing: the raw frames acquired by the high-speed camera (1) are converted to 8-bit grayscale images and processed to eliminate flickering and background, and to isolate the bubbles (2). A threshold is then applied to create binary images (3). At this stage, dilation and erosion algorithms may be applied to eliminate any artefacts created by the binarization. By drawing a measurement line just above the active orifices, it is possible to identify variation in the pixel intensity. Each peak identifies the time at which a bubble starts to form and detach (i.e., formation time) and the time interval between the onset of two consecutive peaks (i.e., bubble period).

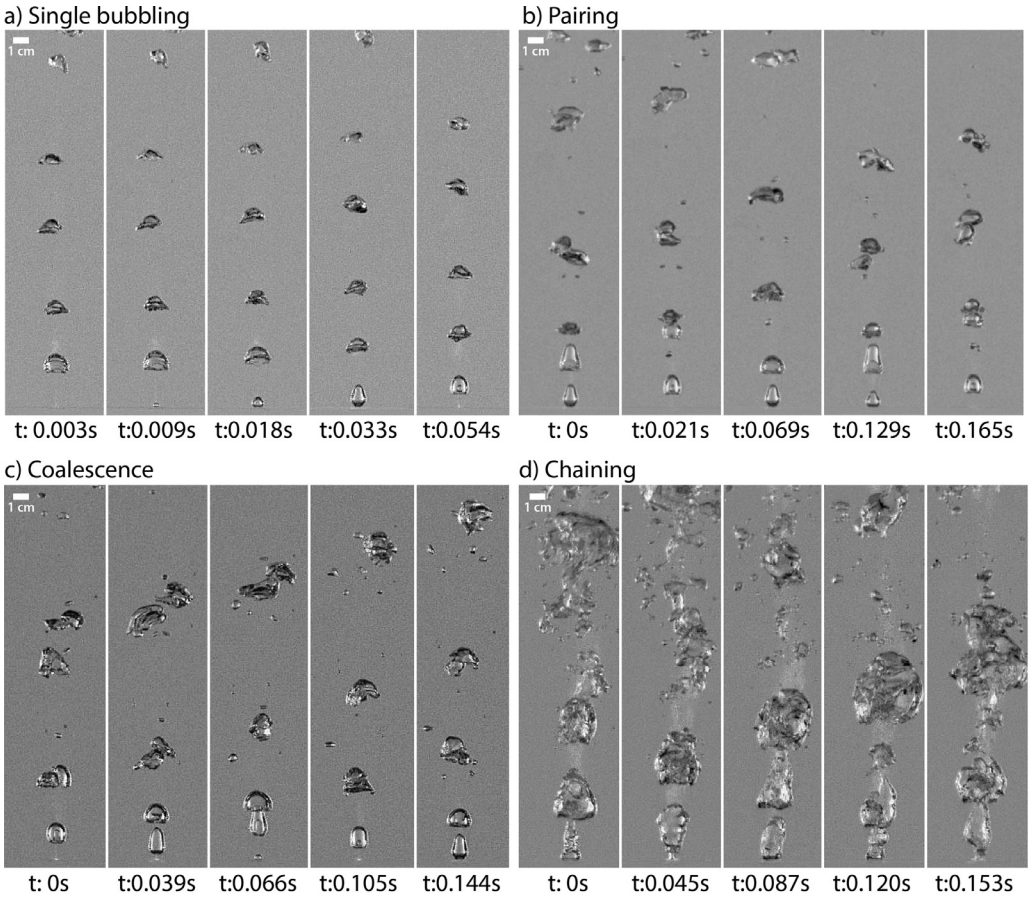

Fig. 4. Experimentally observed bubbling regimes for a single-orifice bubbler, with orifice $D_0 = 2$ mm and $D_b = 2.5$ cm: a) *Single bubbling* ($Q = 0.5$ l/min); b) *Bubbling with pairing* ($Q = 0.8$ l/min); c) *Bubbling with coalescence* ($Q = 1.1$ l/min); and d) *Chaining* ($Q = 10$ l/min).

we modified the threshold values for each stack, to better isolate the bubbles and eliminate spurious pixels around them, created by, e.g., reflections on the glass or variations in illumination conditions. To refine the binary stack, we also used 'Dilation' and 'Erosion' to smooth the bubble edges, and fill in holes in their interiors, created by residual noise present in the stack. Once we obtain a binarized stack, we were able to determine the temporal evolution of pixel level (black = 255 = bubble, white = 0 = no bubble) in the videos along a horizontal line just above the orifices, using the built-in function in Fiji (Fig. 3).

3. Results

3.1. Bubbling regimes in single-orifice bubblers

The behaviour of a bubble emerging from an orifice depends on whether or not it interacts with the wake of the previous bubble to form at that orifice. The growth of a forming bubble may be accelerated through this interaction, and the intensity of interaction between successive bubbles increases with increasing flow rates. We observe the same regimes of bubble formation, as characterized by degree of bubble interaction, as previously described in the literature (e.g., Muller and Prince, 1972; Clift et al., 1978; Badam et al., 2007; Wang et al., 2017). Here, we briefly describe the main features of each regime based on our own observations. We use 'formation time' to indicate the time interval between the onset of bubble formation at an orifice and its detachment, and 'bubble period' to indicate the time interval between the onset of formation of two consecutive bubbles (Fig. 3).

1) *Single bubbling*

Bubbles form singly at the orifice, with regular period, and without interacting with previous or successive bubbles (Fig. 4a). During the formation time, each bubble maintains a spherical shape and, as soon as it detaches from the orifice, it rises buoyantly while deforming irregularly. Bubble volume and period are constant at a given flow rate. As flow rate increases, bubble volume increases, the bubble period becomes shorter (Table 2), and the deformation during ascent becomes more pronounced. The wake generated by the rising bubble doesn't appear to affect the formation and ascent processes of the following bubble.

2) *Bubbling with pairing*

There is some interaction between successive bubbles – two or more bubbles appear to collide, but without coalescence, and rise together as a pair or group (Fig. 4b). After the formation of the leading bubble, its wake causes the next bubble that forms to accelerate so that the two bubbles group together. Once they pair, they rise with a characteristic motion in which they approach and retreat from one another cyclically. As flow rate increases, bubble volume increases and bubble period decreases, but bubble formation time remains constant (Table 2). Higher flow rates promote the formation of three- and four-bubble groups. The bubbles tend to group just above the orifice, and then rise as a bubble raft.

3) *Bubbling with coalescence*

Strong interaction leads to coalescence of two to four bubbles (Fig. 4c). The wake of the lead bubble causes the next bubble to elongate vertically while still forming and accelerates its detachment. This is followed by coalescence of the two bubbles just

Table 2
Single-orifice bubbler bubbling regimes, bubble period (s) and formation time (s).

Gas flow rate (l/min)	D_0		
	1 mm	2 mm	3 mm
		$D_b = 2.5$ cm	
0.2	Pairing	Single bubbling	Single bubbling
0.5	Coalescence	Single bubbling	Single bubbling
0.8	Coalescence	Pairing	Pairing
1.1	Coalescence	Coalescence	Pairing
2	Chaining	Coalescence	Coalescence
3.5	Chaining	Coalescence	Coalescence
5	Chaining	Chaining	Coalescence
10	Jetting	Chaining	Chaining
		$D_b = 1$ cm	
0.2	Pairing	Pairing	Single bubbling
0.5	Pairing	Pairing	Single bubbling
0.8	Coalescence	Pairing	Pairing
1.1	Coalescence	Coalescence	Pairing
2	Chaining	Coalescence	Coalescence
3.5	Chaining	Coalescence	Coalescence
5	Chaining	Chaining	Coalescence
10	Jetting	Chaining	Chaining
		$D_b = 0.7$ cm	
0.2	Single bubbling	Single bubbling	No bubbling
0.5	Pairing	Single bubbling	No bubbling
0.8	Coalescence	Pairing	Single bubbling
1.1	Coalescence	Coalescence	Single bubbling
2	Chaining	Coalescence	Pairing
3.5	Chaining	Coalescence	Coalescence
5	Chaining	Coalescence	Coalescence
10	Jetting	Chaining	Coalescence
	$D_b = 2.5$ cm – Bubble period (s)/formation time (s)		
0.2	0.024–0.126/0.021	0.222/0.033	0.111/0.03
0.5	0.024/0.02	0.099/0.03	0.111/0.03
0.8	0.0216/0.02	0.069/0.03	0.084/0.03
1.1	0.021/0.022	0.057/0.03	0.080/0.03
2	Continuous/Continuous	0.047/0.03	0.045/0.03
3.5	Continuous/Continuous	0.035/0.03	0.048/0.034
5	Continuous/Continuous	0.03/0.03	0.034/0.036
10	Continuous/Continuous	Continuous/0.021	Continuous/0.036
	$D_b = 1$ cm – Bubble period (s)/formation time (s)		
0.2	0.024–0.078/0.021	0.09–0.036/0.018–0.033	0.096/0.042
0.5	0.024/0.0185	0.06–0.048/0.033	0.075/0.036
0.8	0.021/0.0156	0.024–0.042/0.024–0.033	0.069/0.036
1.1	0.021/0.012	0.048/0.03	0.057/0.036
2	Continuous/0.012–0.015	0.048/0.03	0.03–0.036/0.027–0.03
3.5	Continuous/0.009–0.015	0.032/0.03	0.027–0.048/0.027–0.03
5	Continuous/<0.009	0.03/0.018–0.03	0.018–0.048/0.015–0.03
10	Continuous/Stream	Continuous/<0.02	Continuous/0.015–0.03
	$D_b = 0.7$ cm – Bubble period (s)/formation time (s)		
0.2	0.174/0.027	0.093/0.03	–/–
0.5	0.099/0.027	0.063/0.03	–/–
0.8	0.081/0.021	0.042/0.03	0.024/0.045
1.1	0.069/0.021	0.015–0.033/0.018–0.03	0.024/0.036
2	Continuous/0.018	0.018–0.036/0.015–0.036	0.045/0.036
3.5	Continuous/0.015	0.012–0.03/0.015–0.03	0.03–0.042/0.027–0.036
5	Continuous/<0.015	0.009–0.027/0.009–0.03	0.021–0.045/0.024–0.042
10	Continuous/Stream	Continuous/<0.2	0.012–0.045/0.015–0.03

above the orifice. The bubble formation time is generally lower than for the pairing regime (Table 2). As flow rate increases, bubble volume increases, bubble period decreases, and the number of bubbles that coalesce increases up to a maximum of four, as also observed by Wang et al. (2017). Just after coalescence, the coalesced bubble breaks up into smaller bubbles again, which either coalesce again to rise as single large bubble, or group together as a bubble raft. Often this break-up process results in small satellite bubbles that rise with the main bubble.

4) *Chaining*

Four or more bubbles rapidly coalesce at the orifice, forming a continuous chain that connects to a large leading bubble (Fig. 4d). The number of bubbles involved, their size, and the chain height, increase for increasing flow rates; the chain may be few cm high (~5 cm) at the lower flow rates, up to ~17–20 cm for the highest flow rates. The leading bubble rises rapidly following detachment, and its wake causes the following bubbles to elongate as soon as they start to form, so that the bubble tip is sucked into the wake of the previous bubble and coalescence often occurs before detachment. Consequently, it is often not possible to identify a formation time or bubble period. During the entire process, the chain moves upwards rapidly as a continuous gas body. If the chain breaks, it then reconnects rapidly, generating several smaller satellite bubbles in the surrounding liquid.

5) *Jetting*

At the highest flow rate, air flows continually from the orifice with chaotic behaviour (Fig. 5). A central main plume of air is

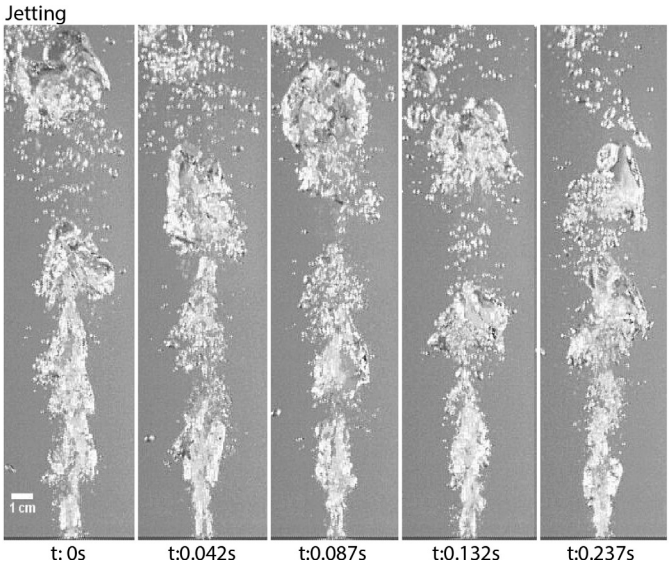

Fig. 5. Experimentally observed *Jetting* regime for single-orifice bubbler, with orifice $D_0 = 1$ mm, $D_b = 0.7$ cm, and $Q = 10$ l/min.

surrounded by smaller bubbles that form at the gas-liquid interface. Formation time and period cannot be determined. At the top of the plume it may be possible to observe occasional breaking and coalescence of large, deformed bubbles that detach from the main jet.

3.1.1. Effect of orifice diameter and bubbler volume

We observe the same regimes described above for different orifice diameter and bubbler volume, but at different flow rates (Table 2). Orifice and bubbler diameter have an important role in controlling bubble properties, period and formation time.

The size of the bubbles depends on the flow conditions. Bubbles forming under constant-pressure conditions are generally larger than those forming under constant-flow conditions, and those forming under intermediate conditions have a size that is intermediate between the two other regimes (Clift et al., 1978). We observe this clearly in single bubbling experiments that cover all three regimes (Fig. 2). For example, $Q = 0.2$ l/min and $D_0 = 2$ mm gives constant-pressure, intermediate, and constant-flow conditions for $D_b = 2.5$, 1.0, and 0.7 cm respectively. By measuring the diameter of the bubble at the moment of detachment (D_{bubble}) and assuming spherical shape, we obtain volumes of ~0.45, ~0.25 and ~0.15 cm^3 for $D_b = 2.5$, 1.0, and 0.7 cm respectively (measured D_{bubble} of ~0.95, ~0.78 and ~0.66 cm, Table 3). In the single bubbling regime, bubble size also increases as orifice diameter increases, for constant bubbler diameter and flow rate, as reported in the literature (e.g., Clift et al., 1978; Tsuge and Hibino, 1983).

It is more complicated to determine variations in volume and formation time for the pairing and coalescence regimes, which are characterized by higher flow rates. In these regimes the wake of the leading bubble accelerates the detachment of the following bubbles, which are then usually smaller than the leading bubble, as also observed by Tsuge and Hibino (1983) and Chakraborty et al. (2015). Generally, for larger bubbler diameter (2.5 cm and 1 cm) and fixed flow rate, both bubble formation time and period tend to increase with increasing orifice diameter. For the smaller bubbler diameter (0.7 cm), we observe more variability: increasing orifice diameter from 1 to 2 mm leads to a decrease in bubble period, while bubble formation time increases; for the bigger orifice diameter (3 mm), bubble period increases again while the formation time remains stable. Fewer bubbles are released faster, and the bubbles are smaller, for a larger orifice diameter.

Table 3
Measured bubble diameters for different flow regimes, in single- and multi-orifice bubblers (CP: constant-pressure conditions; IC: intermediate-flow conditions; CF: constant-flow conditions).

System configuration	D_b (cm)	Flow regime	D_{bubble} (cm)
$N = 1,\ Q = 0.2\ l/min,\ D_0 = 2\ mm$	2.5	CP	~0.95
	1	IC	~0.78
	0.7	CF	~0.66
$N = 3,\ Q = 0.2\ l/min,\ D_0 = 1\ mm$	2.5	CP	~0.72
	1	IC	~0.67
	0.7	CF	~0.61
$N = 3,\ Q = 0.2\ l/min,\ D_0 = 2\ mm$	2.5	IC	~0.79
	1	CF	~0.67
	0.7	CF	~0.67
$N = 5,\ Q = 0.2\ l/min,\ D_0 = 2\ mm$	2.5	IC	~0.70
	1	CF	~0.65
	0.7	CF	~0.63
$N = 9,\ Q = 0.2\ l/min,\ D_0 = 2\ mm$	2.5	IC	~0.60–0.78
	1	CF	~0.42–0.63
	0.7	CF	~0.67

3.2. Bubbling regimes in multi-orifice in-line bubblers

Bubbling behaviour at each orifice of a multi-orifice bubbler can be characterized using the classification described above. For our experiments, bubbling at any orifice was always in the single bubbling, pairing, or coalescence regime – gas flow rates were insufficient to reach the chaining or jetting regime for multiple orifices. A more important metric for describing behaviour of the multi-orifice bubbler is the degree of synchronization among the active orifices. We identify five modes of bubbling, which encompass all of the configurations used for the experiments: 1) Solo bubbling, 2) Synchronous, 3) Partly-synchronous, 4) Alternate, and 5) Asynchronous. Tables 4, 5 and 6 illustrate the regimes of bubbling for each bubbler diameter, as a function of number of orifices, orifice spacing, and orifice diameter.

1) *Solo bubbling*

Only one of the open orifices is active and bubbles form singly at the orifice. During the formation time each bubble maintains a spherical shape and, as soon as it detaches from the orifice, it starts to deform irregularly. As flow rate increases, bubble volume increases, bubble formation time decreases, bubble period becomes shorter and bubble deformation becomes more pronounced. Higher flow rates promote the interaction between successive bubbles, and bubbling shifts from single bubbling, to pairing regime, up to bubbling with coalescence (Fig. 6a, b, c respectively). Bubbling never reaches chaining or jetting regimes. For the same gas flow rate, bubbler volume and orifice diameter, 3- and 5-orifice configurations show a longer bubble period and formation time compared to a single-orifice configuration, while for a 9-orifice configuration both bubble period and formation time are shorter than for a single-orifice configuration (Table 7).

2) *Synchronous*

All the open orifices are active and bubbles form simultaneously at each of them, with the same bubble period and formation time (Fig. 7a). As soon as they detach, bubbles rise buoyantly from each orifice, creating well-organized trails of bubbles sharing similar size, position, deformation pattern, velocity and trajectory. The trails maintain a distance between them equal to the orifice spacing. As flow rate increases, bubble size and degree of deformation increase, and bubble period decreases equally at each orifice. Sometimes – and independent of the gas flow rate – one

Table 4
Multi-orifice bubbler bubbling regimes, for $D_b = 2.5$ cm, varying flow rates, number of orifices and spacing ($S1 = 3.5$ cm, $S2 = 7.5$ cm, $S3 = 15$ cm). The numbers in brackets indicate the active orifices for each case.

Q (l/min)	3 orifices			5 orifices			9 orifices
	S1	S2	S3	S1	S2	S3	–
				$D_b = 2.5$ cm, $D_O = 1$ mm			
0.2	Partly synch.	Partly synch.	Partly synch.	Partly synch. (4)	Partly synch. (4)	Partly synch. (4)	Partly synch. (5)
0.5	Partly synch.	Partly synch.	Alternate (all)	Partly synch. (all)	Partly synch. (4)	Partly synch. (4)	Partly synch. (6)
0.8	Alternate (all)	Alternate (all)	Alternate (all)	Partly synch. (all)	Partly synch. (4)	Partly synch. (4)	Partly synch. (7)
1.1	Alternate (all)	Alternate (all)	Asynch. (all)	Alternate (all)	Partly synch. (4)	Partly synch. (4)	Partly synch. (7)
2	Asynch. (all)	Asynch. (all)	Asynch. (all)	Alternate (all)	Alternate (all)	Alternate (all)	Alternate (all)
3.5	Asynch. (all)	Asynch. (all)	Asynch. (all)	Asynch. (all)	Alternate (all)	Alternate (all)	Alternate (all)
5	Asynch. (all)	Asynch. (all)	Asynch. (all)	Asynch. (all)	Alternate (all)	Asynch. (all)	Asynch. (all)
10	Asynch. (all)	Asynch. (all)	Asynch. (all)	Asynch. (all)	Alternate (all)	Asynch. (all)	Asynch. (all)
				$D_b = 2.5$ cm, $D_O = 2$ mm			
0.2	Solo (1)	Partly synch. (all)	Partly synch. (2)	Partly synch. (4)	Partly synch. (2)	Partly synch. (3)	Partly synch. (3)
0.5	Partly synch (all)	Partly synch. (all)	Partly synch. (2)	Partly synch. (4)	Partly synch. (2)	Partly synch. (3)	Partly synch. (3)
0.8	Partly synch (all)	Partly synch. (all)	Partly synch. (all)	Partly synch. (4)	Partly synch. (3)	Partly synch. (4)	Partly synch. (5)
1.1	Alternate (all)	Alternate (all)	Alternate (all)	Partly synch. (all)	Partly synch. (all)	Alternate (all)	Partly synch. (7)
2	Alternate (all)	Alternate (all)	Alternate (all)	Alternate (all)	Alternate (all)	Alternate (all)	Partly synch. (7)
3.5	Alternate (all)	Alternate (all)	Alternate (all)	Alternate (all)	Alternate (all)	Alternate (all)	Alternate (all)
5	Asynch. (all)	Alternate (all)	Alternate (all)	Asynch. (all)	Alternate (all)	Alternate (all)	Alternate (all)
10	Asynch. (all)	Asynch. (all)	Asynch. (all)	Asynch. (all)	Asynch. (all)	Alternate (all)	Alternate (all)
				$D_b = 2.5$ cm, $D_O = 3$ mm			
0.2	Solo (1)	Solo (1)	Solo (1)	Solo (1)	Solo (1)	Solo (1)	Solo (1)
0.5	Solo (1)	Partly synch. (2)	Solo (1)	Solo (1)	Solo (1)	Solo (1)	Solo (1)
0.8	Partly synch. (3)	Partly synch. (all)	Solo (1)	Partly synch. (all)	Solo (1)	Partly synch. (2)	Partly synch. (2)
1.1	Partly synch. (3)	Partly synch. (all)	Partly synch. (2)	Partly synch. (all)	Partly synch. (2)	Partly synch. (2)	Partly synch. (2)
2	Partly synch. (all)	Partly synch. (all)	Partly synch. (all)	Partly synch. (all)	Partly synch. (all)	Partly synch. (all)	Partly synch. (6)
3.5	Alternate (all)	Alternate (all)	Alternate (all)	Alternate (all)	Partly synch. (all)	Alternate (all)	Partly synch. (7)
5	Alternate (all)	Alternate (all)	Alternate (all)	Alternate (all)	Alternate (all)	Alternate (all)	Alternate (all)
10	Asynch. (all)	Asynch. (all)	Alternate (all)	Alternate (all)	Alternate (all)	Alternate (all)	Alternate (all)

Table 5
Multi-orifice bubbler bubbling regimes, for $D_b = 1$ cm, varying flow rates, number of orifices and spacing ($S1 = 3.5$ cm, $S2 = 7.5$ cm, $S3 = 15$ cm). The numbers in brackets indicate the active orifices for each case.

Q (l/min)	3 orifices			5 orifices			9 orifices
	S1	S2	S3	S1	S2	S3	–
				$D_b = 1$ cm, $D_O = 1$ mm			
0.2	Partly synch. (2)	Partly synch. (2)	Solo (1)	Partly synch. (2)	Partly synch. (2)	Solo (1)	Solo
0.5	Partly synch. (2)	Synch. (All)	Partly synch. (2)	Partly synch. (3)	Partly synch. (3)	Partly synch. (4)	Partly synch. (4)
0.8	Partly synch. (2)	Synch. (All)	Alternate (all)	Partly synch. (4)	Synch. (all)	Partly synch. (4)	Partly synch. (7)
1.1	Alternate (all)	Alternate (all)	Alternate (all)	Alternate (4)	Synch. (all)	Synch. (all)	Partly synch. (all)
2	Alternate (all)	Alternate (all)	Alternate (all)	Alternate (all)	Alternate (all)	Alternate (all)	Alternate (all)
3.5	Alternate (all)	Alternate (all)	Asynch. (all)	Alternate (all)	Alternate (all)	Alternate (all)	Alternate (all)
5	Asynch. (all)	Asynch. (all)	Asynch. (all)	Asynch. (all)	Alternate (all)	Alternate (all)	Alternate (all)
10	Asynch. (all)	Asynch (all)	Asynch. (all)	Asynch. (all)	Alternate (all)	Asynch. (all)	Asynch. (all)
				$D_b = 1$ cm, $D_O = 2$ mm			
0.2	Solo (1)	Solo (1)	Solo (1)	Partly synch. (2)	Solo (1)	Solo (1)	Partly synch. (3)
0.5	Partly synch. (2)	Solo (1)	Solo (1)	Partly synch. (2)	Partly synch. (2)	Partly synch. (2)	Partly synch. (3)
0.8	Partly synch. (all)	Solo (1)	Partly synch. (2)	Partly synch. (4)	Partly synch. (3)	Partly synch. (2)	Partly synch. (4)
1.1	Partly synch. (all)	Partly synch. (all)	Partly synch. (2)	Partly synch. (all)	Partly synch. (3)	Synch. (2)	Partly synch. (5)
2	Synch. (all)	Synch. (all)	Partly synch. (all)	Alternate (all)	Synch. (4)	Synch. (4)	Partly synch. (7)
3.5	Asynch (all)	Alternate (all)	Alternate (all)	Alternate (all)	Alternate (4)	Alternate (4)	Alternate (all)
5	Asynch. (all)	Alternate (all)	Asynch. (all)	Alternate (all)	Alternate (all)	Alternate (all)	Alternate (all)
10	Asynch (all)	Asynch. (all)	Asynch. (all)	Asynch. (all)	Alternate (all)	Alternate (all)	Asynch. (all)
				$D_b = 1$ cm, $D_O = 3$ mm			
0.2	Solo (1)	Solo (1)	Solo (1)	Solo (1)	Solo (1)	Solo (1)	Solo (1)
0.5	Solo (1)	Solo (1)	Solo (1)	Solo (1)	Solo (1)	Solo (1)	Solo (1)
0.8	Solo (1)	Solo (1)	Partly synch. (2)	Solo (1)	Solo (1)	Solo (1)	Solo (1)
1.1	Solo (1)	Solo (1)	Partly synch. (2)	Solo (1)	Solo (1)	Partly synch. (2)	Partly synch. (2)
2	Partly synch. (all)	Partly synch. (2)	Partly synch. (all)	Partly synch. (2)	Partly synch. (4)	Partly synch. (3)	Partly synch. (3)
3.5	Alternate (all)	Alternate (all)	Synch. (all)	Partly synch. (4)	Partly synch. (4)	Partly synch. (4)	Partly synch. (5)
5	Alternate (all)	Alternate (all)	Alternate (all)	Alternate (4)	Partly synch. (4)	Alternate (4)	Partly synch. (5)
10	Asynch. (all)	Alternate (all)	Asynch. (all)	Alternate (all)	Alternate (all)	Alternate (all)	Alternate (all)

(or more) orifice may produce bigger bubbles than the other orifices. The wake generated by the rising bubbles does not affect the formation and ascent processes of the following bubble, and there are no pairing or coalescence events. Fig. 8a shows how, for a 3-orifice configuration, bubble period and formation time are fully synchronous among the orifices.

3) *Partly-synchronous*

Only a subset of the open orifices is active synchronously, forming bubbles with equal bubble period and formation time, while the others remain inactive (Fig. 7b). Similarly to the Synchronous regime, after detachment the bubbles rising from the active orifices create trails characterized by the same bubble shape, position,

Table 6
Multi-orifice bubbler bubbling regimes, for $D_b = 0.7$ cm, varying flow rates, number of orifices and spacing ($S1 = 3.5$ cm, $S2 = 7.5$ cm, $S3 = 15$ cm). The numbers in brackets indicate the active orifices for each case.

Q (l/min)	3 orifices			5 orifices			9 orifices
	S1	S2	S3	S1	S2	S3	–
				$\boldsymbol{D_b = 0.7}$ **cm,** $\boldsymbol{D_O = 1}$ **mm**			
0.2	Partly synch. (2)	Solo (1)	Synch. (all)	Solo (1)	Solo (1)	Partly synch. (2)	Partly synch. (2)
0.5	Synch. (all)	Partly synch. (2)	Alternate (2)	Partly synch. (4)	Synch. (all)	Partly synch. (3)	Partly synch. (4)
0.8	Synch. (all)	Alternate (all)	Alternate (all)	Partly synch. (4)	Partly synch. (3)	Partly synch. (4)	Partly synch. (4)
1.1	Alternate (all)	Alternate (all)	Alternate (all)	Partly synch. (4)	Partly synch. (all)	Alternate (4)	Partly synch. (6)
2	Alternate (all)	Alternate (all)	Alternate (all)	Alternate (4)	Alternate (all)	Alternate (all)	Alternate (all)
3.5	Asynch. (all)	Asynch. (all)	Alternate (all)	Alternate (all)	Alternate (all)	Alternate (all)	Alternate (all)
5	Asynch. (all)	Asynch. (all)	Asynch. (all)	Alternate (all)	Alternate (all)	Alternate (all)	Alternate (all)
10	Asynch. (all)	Asynch. (all)	Asynch. (all)	Asynch. (all)	Asynch. (all)	Asynch. (all)	Asynch. (all)
				$\boldsymbol{D_b = 0.7}$ **cm,** $\boldsymbol{D_O = 2}$ **mm**			
0.2	Solo (1)	Solo (1)	Solo (1)	Solo (1)	Solo (1)	Solo (1)	Solo (1)
0.5	Solo (1)	Partly synch. (2)	Solo (1)	Partly synch. (2)	Partly synch. (2)	Partly synch. (3)	Partly synch. (3)
0.8	Solo (1)	Partly synch. (2)	Partly synch. (2)	Partly synch. (2)	Partly synch. (3)	Partly synch. (3)	Partly synch. (3)
1.1	Alternate (2)	Partly synch. (2)	Partly synch. (2)	Partly synch. (2)	Partly synch. (3)	Partly synch. (3)	Partly synch. (6)
2	Alternate (all)	Partly synch. (2)	Synch. (all)	Partly synch. (4)	Partly synch. (4)	Partly synch. (4)	Partly synch. (7)
3.5	Alternate (all)	Alternate (all)	Alternate (all)	Alternate (all)	Alternate (all)	Alternate (all)	Alternate (all)
5	Asynch. (all)	Alternate (all)	Alternate (all)	Asynch. (all)	Alternate (all)	Alternate (all)	Alternate (all)
10	Asynch. (all)	Asynch. (all)	Asynch. (all)	Asynch. (all)	Alternate (all)	Asynch. (all)	Alternate (all)
				$\boldsymbol{D_b = 0.7}$ **cm,** $\boldsymbol{D_O = 3}$ **mm**			
0.2	NO Bubbling	NO Bubbling	NO Bubbling	NO Bubbling	NO Bubbling	NO Bubbling	NO Bubbling
0.5	NO Bubbling	NO Bubbling	Solo (1)	NO Bubbling	Solo (1)	Solo (1)	NO Bubbling
0.8	Solo (1)	Solo (1)	Solo (1)	Solo (1)	Solo (1)	Solo (1)	NO Bubbling
1.1	Solo (1)	Solo (1)	Solo (1)	Solo (1)	Solo (1)	Solo (1)	Solo (1)
2	Partly synch. (2)	Solo (1)	Synch. (2)	Partly synch. (2)	Solo (1)	Synch. (2)	Solo (1)
3.5	Alternate (2)	Alternate (all)	Synch. (2)	Partly synch. (3)	Synch. (2)	Partly Synch. (4)	Partly synch. (3)
5	Alternate (2)	Alternate (all)	Synch. (all)	Alternate (3)	Alternate (4)	Alternate (all)	Partly synch. (4)
10	Alternate (all)	Alternate (all)	Alternate (all)	Alternate (all)	Alternate (all)	Alternate (all)	Alternate (all)

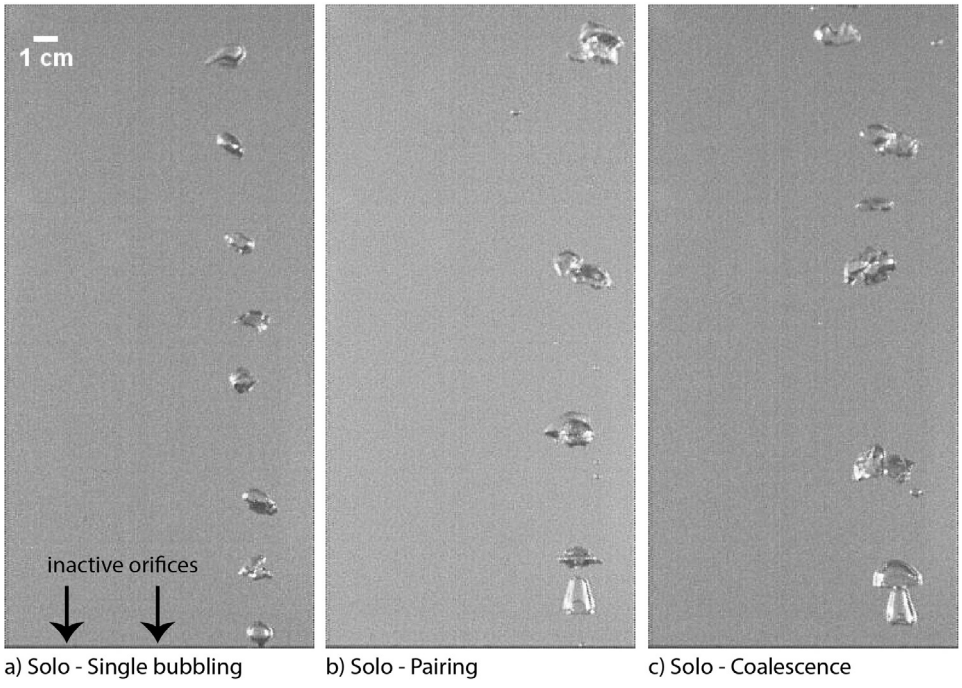

Fig. 6. Experimentally observed bubbling sub-regimes characterizing the main Solo bubbling regime for multi-orifice configurations, with $D_O = 3$ mm and $D_b = 1$ cm. The arrows indicate the position of two open but inactive orifices, next to the active one: a) Solo bubbling - Single bubbling ($Q = 0.5$ l/min); b) Solo bubbling - Bubbling with pairing ($Q = 0.8$ l/min); c) Solo bubbling - Bubbling with coalescence ($Q = 1.1$ l/min).

velocity and trajectory. As flow rate increases, bubble volume increases, and bubble period becomes shorter. The number of active orifices increases as well. A minimum of two orifices form bubbles simultaneously and constantly (i.e., constantly-active). The remaining orifices may be active only intermittently (i.e., partially-active), forming bubbles impulsively with activity switching randomly from orifice to orifice. Whenever the activity switches from one orifice to the other, the newly active orifice shares the same bubbling mode as the previous one that – at the same time – becomes inactive. The activity from the partially-active orifices is always synchronous with the constantly-active orifices. As flow rate further increases, bubble interaction increases equally among all the active orifices, where the same number of bubbles pair or coalesce. Fig. 8b shows, for a 3-orifices configuration, how the two

Table 7
Comparison between bubble period (s) and formation time (s) for single- and multiple-orifice configurations.

Configuration	multi-orifice				single-orifice
	Q (l/min)	Orifices open/active	Spacing (cm)	Bubble period/formation time (s)	Bubble period/formation time (s)
$D_b = 0.7$ cm, $D_O = 1$ mm	0.2	3/2	3.5	0.297/0.03	0.174/0.027
$D_b = 0.7$ cm, $D_O = 1$ mm	0.2	5/1	3.5	0.222/0.03	0.174/0.027
$D_b = 0.7$ cm, $D_O = 1$ mm	0.2	5/1	7.5	0.108/0.03	0.174/0.027
$D_b = 1$ cm, $D_O = 2$ mm	0.2	3/1	15	0.096/0.039	0.09/0.033
$D_b = 1$ cm, $D_O = 2$ mm	0.2	3/1	3.5	0.093/0.036	0.09–0.036/0.018–0.033
$D_b = 0.7$ cm, $D_O = 2$ mm	0.2	9/1	–	0.075/0.03	0.093/0.03
$D_b = 1$ cm, $D_O = 3$ mm	1.1	5/1	3.5	0.06/0.03	0.057/0.036
$D_b = 0.7$ cm, $D_O = 3$ mm	1.1	9/1	–	0.096/0.03	0.24/0.036
$D_b = 2.5$ cm, $D_O = 3$ mm	0.5	9/1	–	0.066/0.027	0.111/0.03

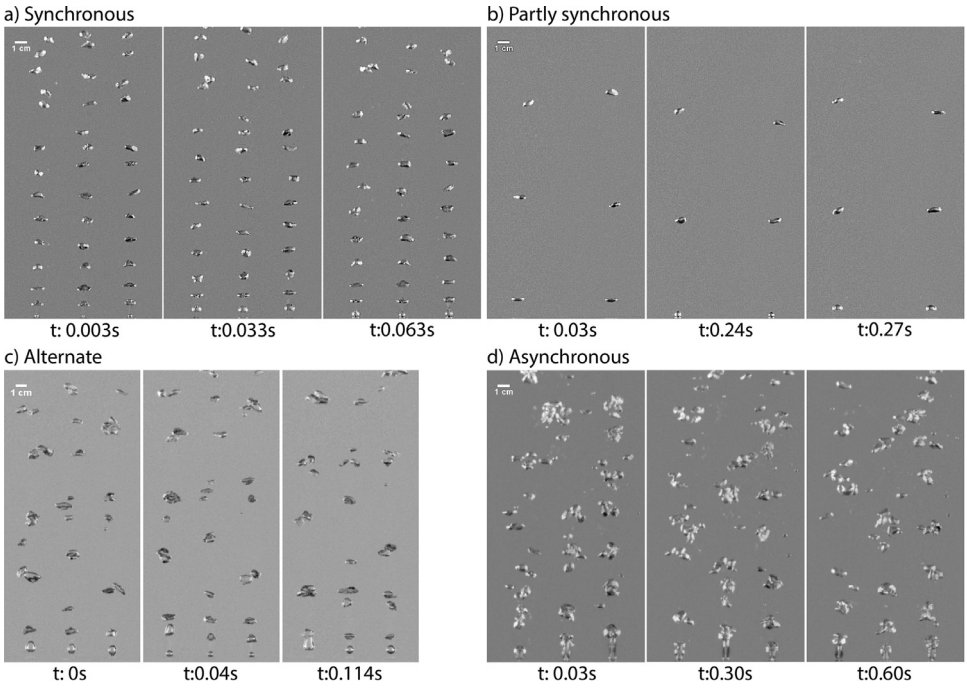

Fig. 7. Experimentally observed bubbling regimes for multi-orifice bubblers: a) *Synchronous* ($D_O = 1$ mm, $D_b = 0.7$ cm, $Q = 0.8$ l/min, $S = 3.5$ cm); b) *Partly synchronous* ($D_O = 1$ mm, $D_b = 0.7$ cm, $Q = 0.2$ l/min, $S = 3.5$ cm); c) *Alternate* ($D_O = 2$ mm, $D_b = 2.5$ cm, $Q = 1.1$ l/min, $S = 3.5$ cm); d) *Asynchronous* ($D_O = 1$ mm, $D_b = 0.7$ cm, $Q = 2$ l/min, $S = 3.5$ cm).

active orifices share the same bubble period and formation time while the third, central orifice is inactive.

4) *Alternate*

The degree of synchronicity among the active orifices gradually decreases as flow rate increases, and bubbling becomes less steady (Fig. 7c). This regime is not always straightforward to distinguish from the Synchronous or Partly-synchronous regimes. However, in the synchronous regimes, at any position above the orifices, the bubbles rise creating well-organized layers of bubbles of similar size and position. Any out-of-phase bubbling creates more unstable layers above the active orifices, with bubbles rising with slightly different ascent time, size and degree of deformation. The greater the distance from the point of origin, the more pronounced the differences from the emission points. Similar to the Partly-synchronous regime, increasing flow rate can increase the number of active orifices. When not all the open orifices are constantly-active, the partially-active ones may form bubbles intermittently, with their activity switching from orifice to orifice and always characterized by a slight time-offset between them. As flow rate increases, bubbling modes at the active orifices move from single-bubbling to bubbling with pairing or coalescence, and the level of synchronicity decreases. Out-of-phase bubbling is well represented in Fig. 8c, where the peaks from each orifice start to lose synchronicity, although the formation time for each bubble remains relatively stable.

5) *Asynchronous*

At any given time, bubbles at active orifices are in a different stage of formation, and there is no synchronicity among orifices (Fig. 7d). Pairing and coalescence above the orifices is also asynchronous, and bubbles are chaotically distributed above the

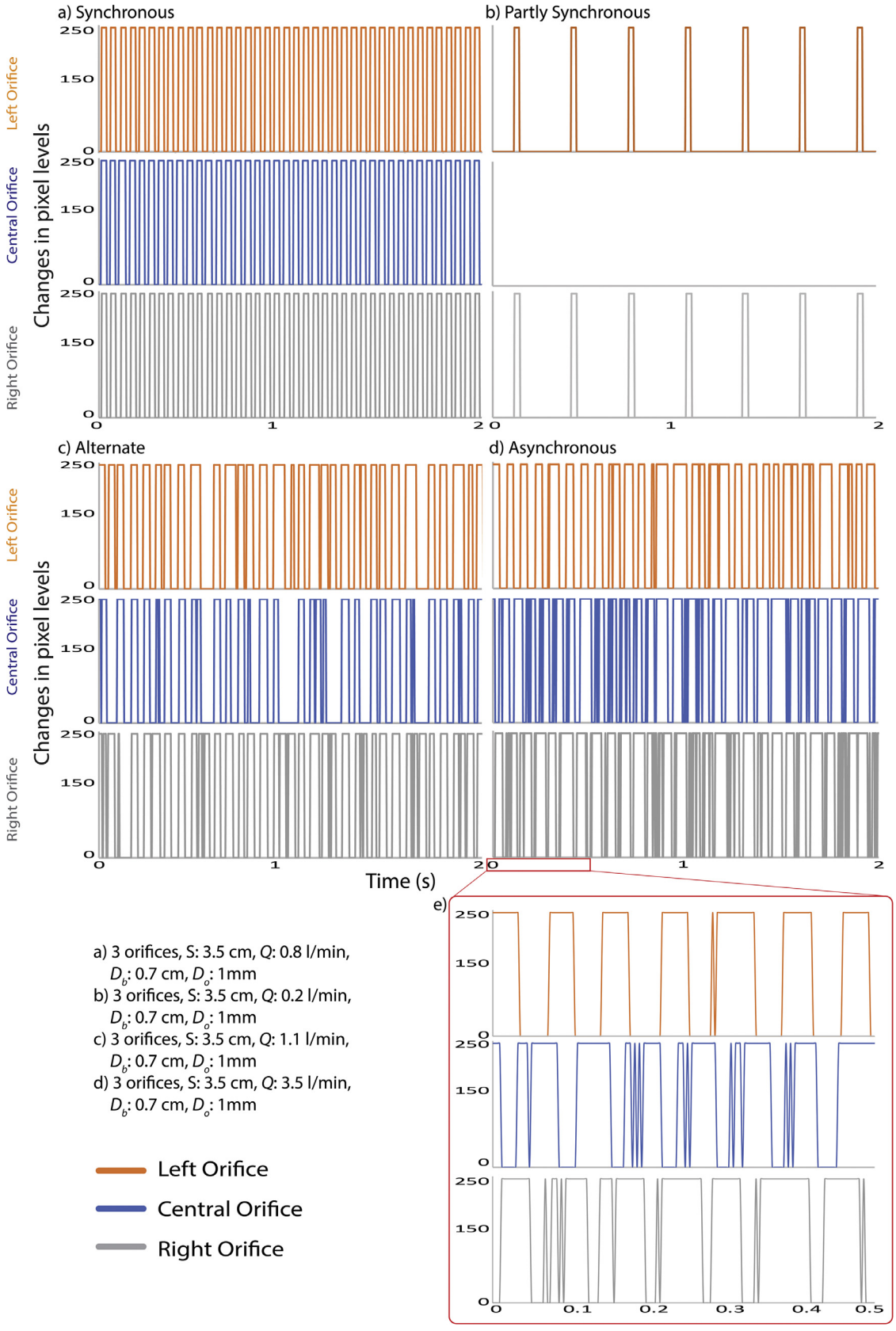

Fig. 8. Comparison of bubble period and formation time at each of the active orifices for a three-orifice bubbler in the a) Synchronous, b) Partly-synchronous, c) Alternate and d) Asynchronous bubbling regimes. In all cases, each orifice is identified by a different colour. When the peaks are fully (a) or partly (b) synchronous, they align closely, sharing the same bubble period, timing and formation time. As synchronicity decreases, the alignment among the peaks decreases (c), until bubbling becomes chaotic (d) and each orifice is characterized by its own bubble period and formation time. The inset in (e) shows details of the first 0.5 s of bubbling, highlighting how chaotic bubbling may become in the Asynchronous regime.

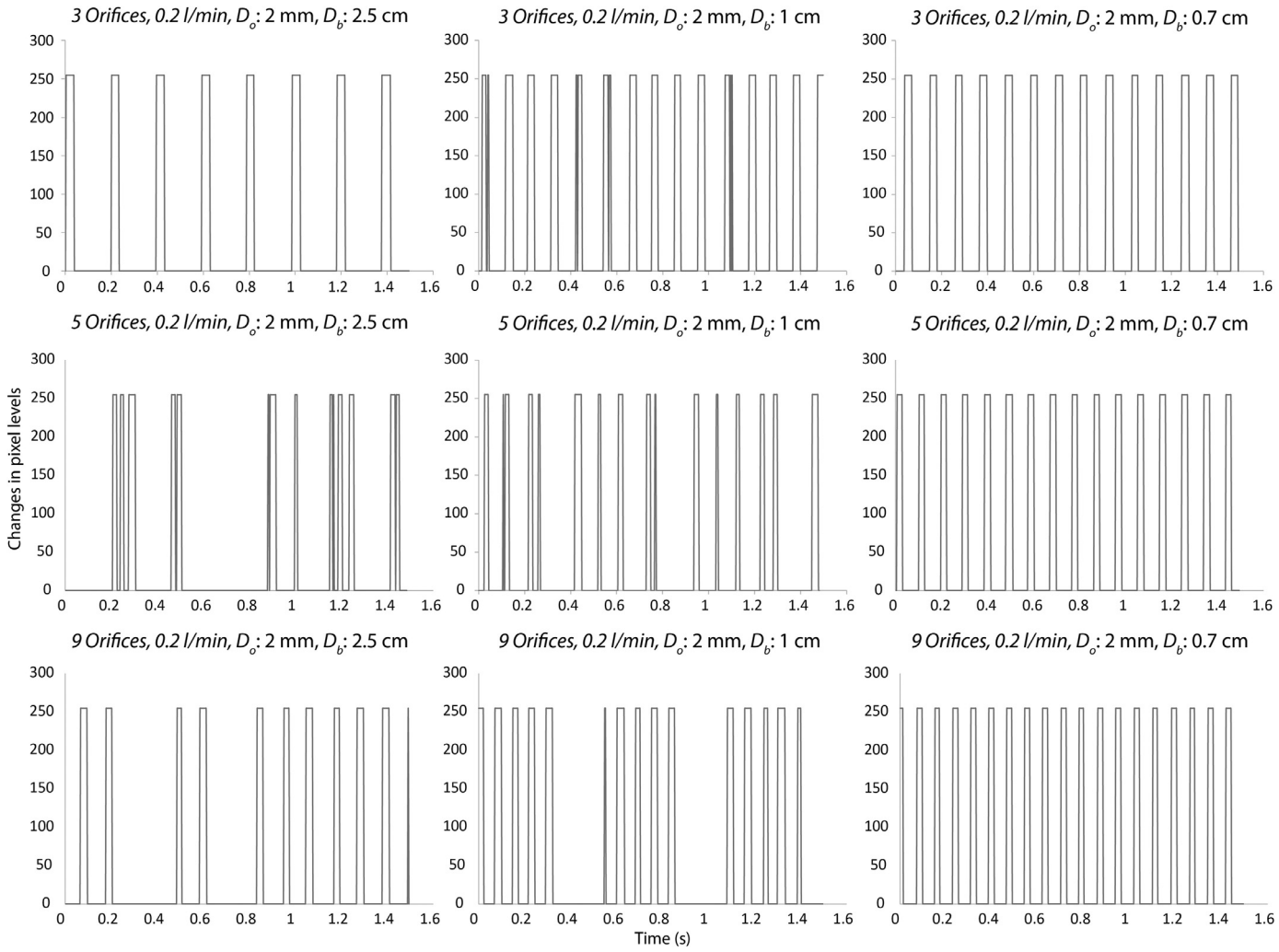

Fig. 9. Effects of bubbler volume on bubble period. For the same flow rate, orifice diameter and spacing, a decrease in the bubbler diameter leads to more regular bubble period at the active orifices. This is particularly true for 5- and 9-orifices configurations.

bubbler, up to the liquid surface. As with the previous regimes, some orifices may be inactive or only active intermittently. As flow rate increases, the bubbling becomes less synchronous, and interaction among bubbles increases. Both pairing and coalescence regimes can occur at different orifices at the same time. Fig. 8d shows the asynchronicity among 3 active orifices, with peaks from each orifice characterized by different bubble period and formation time.

3.2.1. Effect of orifice diameter, number of orifices, and bubbler volume

We observe the same bubbling regimes described above for different orifice diameter, number and spacing, different bubbler volume, and at different flow rates (Tables 4, 5, 6). As a general trend, Solo bubbling occurs for the lower flow rates. As flow rate increases, more orifices become active. A low flow rate favours Synchronous and Partly-synchronous regimes; intermediate flow rates promote Alternate bubbling; and at higher flow rates, the orifices become Asynchronous and bubbling becomes chaotic. Regardless of orifice number, diameter and spacing, as gas flow rate increases, bubbling begins first at one of the outer orifices, and the other outer orifice is the next to become active. Further increase in flow rate activates the orifices sequentially towards the centre, alternating from one end to the other, and the central orifice is always the last to become active.

For 3- and 5-orifice configurations, spacing doesn't affect the bubbling dynamics. This is in contrast to the findings of Ruzicka et al. (2000) and Xie and Tan (2003), who observed a significant increase in degree of bubbling synchronicity for widely spaced orifices, over a range of gas flow rates ($Q = 0.05 - 0.5$ l/min and $Q = 0 - 0.6$ l/min respectively, $D_O = 1.6$ mm and $V_b = 5 \times 10^{-4}$ m^3; Ruzicka et al., 2000; Xie and Tan, 2003). For our higher range of flow rates, varying orifice diameters, spacing, and smaller bubbler volumes, we observe minor variations in the bubbling regimes, mostly arising from changes in flow rates.

As for the single-orifice case, bubbling from the multi-orifice bubblers spans across constant-flow, intermediate-flow and constant-pressure conditions (Fig. 2). The volume of the bubbles varies depending on bubbler diameter and, by extension, on the flow conditions (Table 3). Changing bubbler diameter also affects bubble period. Fig. 9 shows the bubble period for $D_O = 2$ mm, $Q = 0.2$ l/min, $D_b = 2.5,\ 1,\ 0.7$ cm, for 3-, 5-, and 9-orifices configurations. A decrease in the bubbler diameter, for all the other conditions remaining equal, leads to a shorter bubble period, and makes bubbling more regular. This is clear especially for the 5- and 9-orifice configurations, where bubbling is irregular for the bigger bubbler, but becomes increasingly regular for the smaller bubblers (Fig. 9). Also, for 5- and 9-orifice configurations, bubbling activity switches between active and inactive orifices more frequently for the bigger bubbler that for the smaller bubbler.

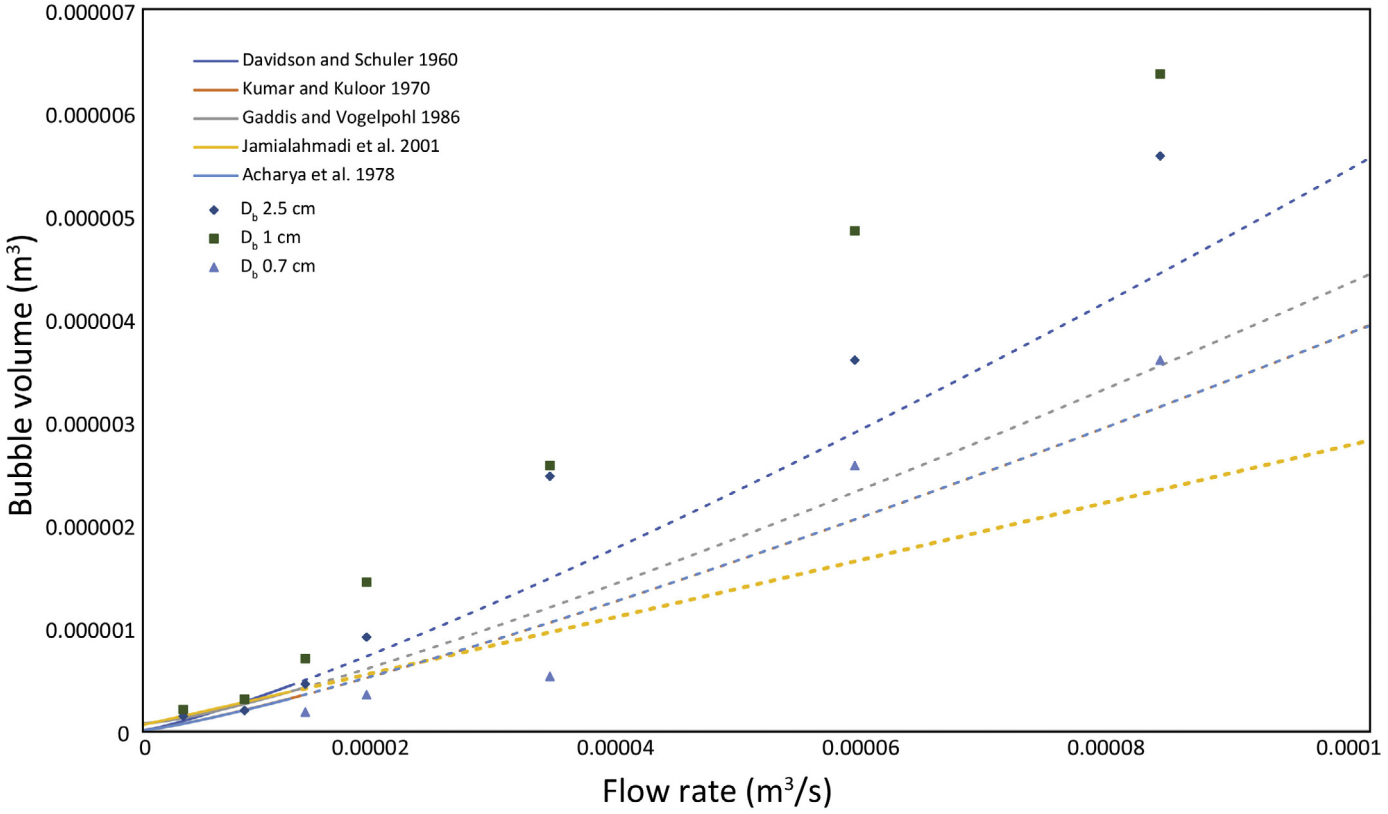

Fig. 10. Volumes for bubbles forming at different gas flow rates in a single orifice bubbler ($D_O = 3$ mm) measured experimentally (symbols) and predicted by different correlations available in literature (lines). Experimental observations agree with model results only for the lower gas flow rates (solid lines). At higher flow rates (dotted lines) the models are not valid anymore, and they either underestimate or – for the smallest bubbler – overestimate bubble volumes.

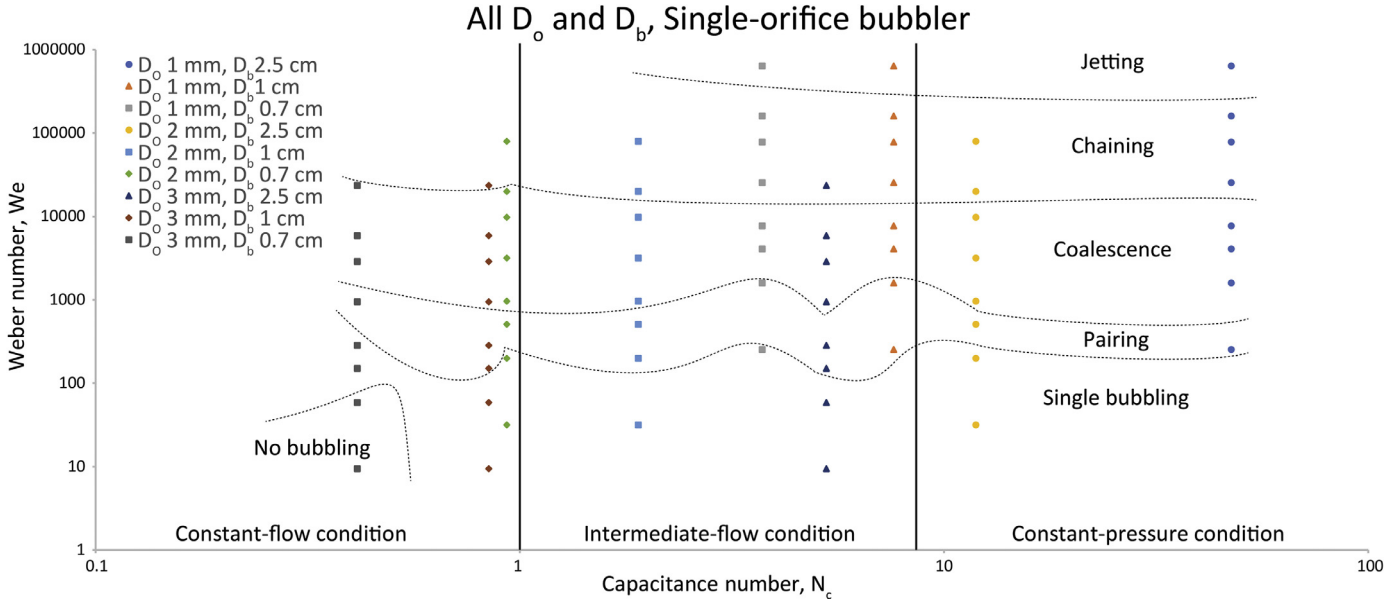

Fig. 11. Bubbling regime map for single-orifice bubblers as a function of the dimensionless capacitance number (N_c) and dimensionless Weber number (We). The dotted lines are drawn to provide a guide to the eye between each bubbling regime. The two vertical blue lines separate the constant-flow, intermediate and constant-pressure conditions. Each symbol colour represents different experimental conditions (bubbler and orifice diameter).

4. Discussion

4.1. Single-orifice bubblers

Bubbling behaviour at a single orifice has been widely investigated, and several physical models have been developed to predict the volume of bubbles forming in the Single bubbling regime, at low and medium flow rates, mainly under the assumptions of constant flow conditions and spherical bubbles (e.g., Davidson and Schueler, 1960a; Kumar and Kuloor, 1970; Acharya et al., 1978; Gaddis and Vogelpohl, 1986; Tsuge et al., 1997; Jamialahmadi et al., 2001). For increasing gas flow rate the models predict a monotonic increase in the bubble volume (Fig. 10). The models agree well with our data at low gas flow rate, when bubbling is in the Single

bubbling regime. However, the models underestimate the size of the bubbles in the Pairing and Coalescence regimes. In the Pairing and Coalescence regimes, interaction between successive bubbles at the orifice increases as gas flow rate increases, and the wake effects influence the bubble volume. As result, a bigger leading bubble is followed by smaller ones, characterized by a shorter formation time. For the Coalescence regime in particular, coalescence events at the orifice become a controlling process in determining the final volume of bubbles: as soon as a bubble forms and detaches from the orifice, a new one grows at the orifice and interacts and coalesces with the previous one, leading to a significant increase in its volume. The higher the gas flow rate, the sooner and closer to the orifice this interaction occurs. The discrepancy between models and experimental data at high gas flow rates demonstrates the need for new models that account for interactions between successive bubbles at the orifice. Results from more recent numerical simulations show qualitative agreement with our experimental observations, predicting that bubble volume and

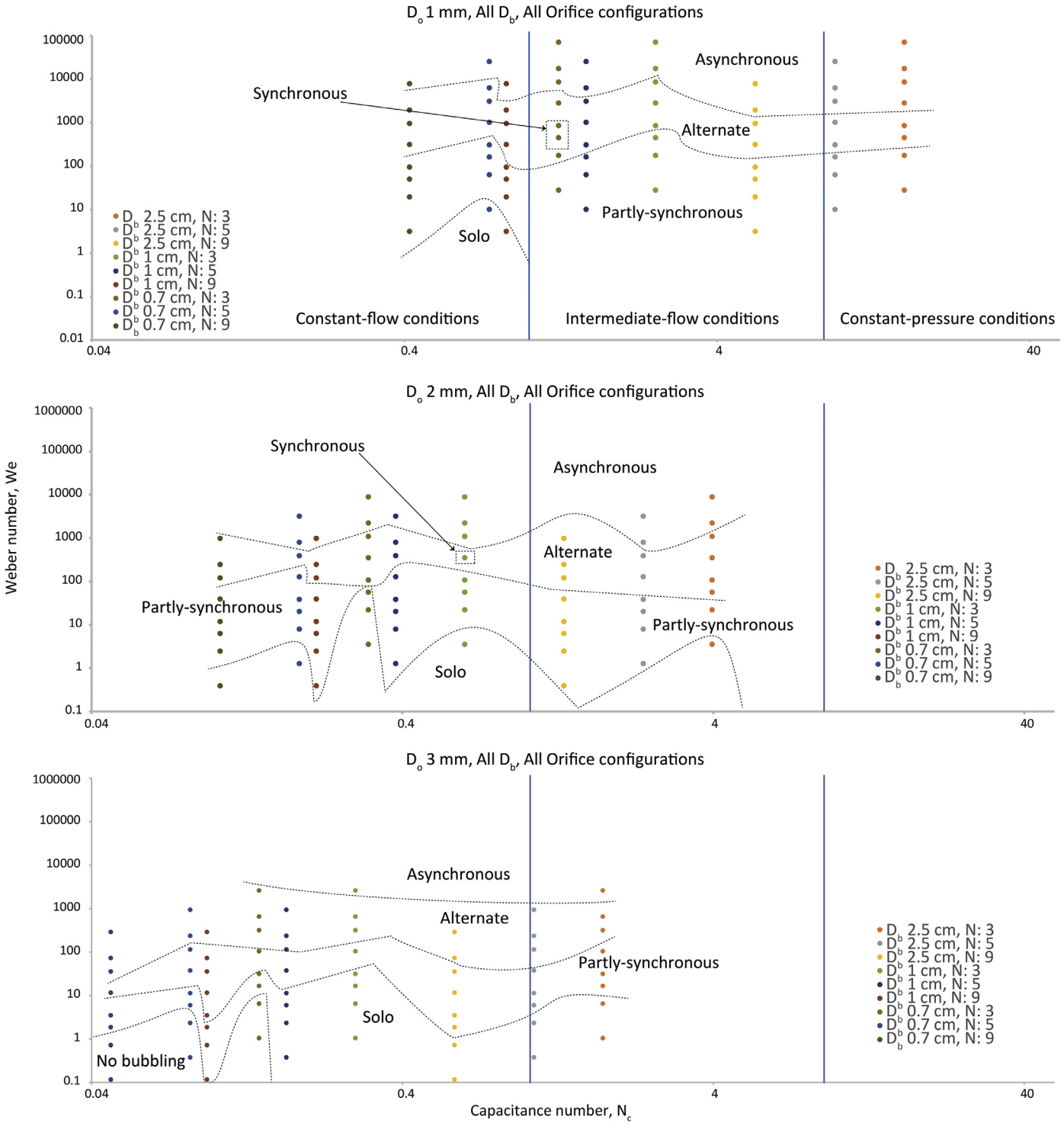

Fig. 12. Bubbling regime maps for orifice diameter of 1 (upper), 2 (central) and 3 (bottom) mm, as function of the dimensionless Capacitance number (N_c) and dimensionless Weber number (We). The dotted lines are drawn to provide a guide to the eye between each bubbling regime. The two vertical blue lines separate the constant-flow, intermediate and constant-pressure conditions. Each circle colour represents different experimental conditions (bubbler diameter, D_b, and number of open orifices, N).

formation time is constant in the Single bubbling regime, but that in the Pairing regime, bubble size and formation time are reduced for the following bubble of a pair (Chakraborty et al., 2015).

Our data show that the bubbling regimes and their transitions are strongly controlled by Weber number, but do not appear to be sensitive to Capacitance number (Fig. 11). As a general trend, Single bubbling occurs for low Weber number ($We \lesssim 250$), with the regime transitioning as Weber number increases through Pairing ($250 \lesssim We \lesssim 1500$), Coalescence ($500 \lesssim We \lesssim 2 \times 10^4$), and Chaining ($1 \times 10^4 \lesssim We \lesssim 1.6 \times 10^5$), reaching jetting conditions only for the highest Weber numbers ($We \gtrsim 6 \times 10^5$). The Weber number dependence indicates that bubbling behaviour is controlled by a competition between inertial and surface tension forces. At low Weber number (small orifice or low gas velocity) the surface tension dominates, and formation of stable, single bubbles is favoured. At high Weber number (large orifice or high gas velocity) inertia dominates favouring interaction and coalescence. Note that our experimental data (Fig. 11) appear to show that larger orifices lead to lower Weber numbers, but this is because, for a given gas flow rate, doubling the orifice diameter reduces gas velocity by a factor of four, hence the change in gas velocity dominates.

4.2. Multi-orifice bubblers

When multiple orifices are active simultaneously, behaviour at any orifice is characterized by the same suite of regimes that are observed in a single-orifice bubbler. However, the bubbling regime may vary from orifice to orifice, and the degree of synchronization among the orifices, and the number of orifices that are active, may also vary (Tables 4–6). Variations in behaviour at different orifices is likely a result of complex interaction among the orifices as they compete for gas, mediated by induced liquid flow. As discussed in the previous section, the wake of a bubble may affect the behaviour of the next bubble produced at the same orifice. Similarly, the repeated ascent of bubbles from an orifice may set up convective cells in the surrounding liquid that affect the behaviour of bubbles forming at adjacent orifices (e.g., Ruzicka et al., 1999). Thus, bubbles may behave as if they were forming in a co-flowing environment rather than in a stagnant liquid (e.g., Sevilla et al., 2005; Chakraborty et al., 2011). Co-flow (i.e. where there is an upward flow of liquid past the orifice) may lead to an increase in the mean distance between successive bubbles at an orifice, thus decreasing the influence of the leading bubble's wake on the formation of the following bubble. This, in turn, may diminish or suppress pairing and coalescence processes. Such dynamics have been observed in single-orifice bubbling both numerically (Chakraborty et al., 2011) and experimentally (Sevilla et al., 2005) where, for the same conditions, pairing and coalescence processes are observed in stagnant liquids, but are suppressed at moderate co-flowing velocities. For a multi-orifice bubbler we may expect that orifices will interact less strongly when they are more widely spaced (e.g., Ruzicka et al., 1999). In some cases, our data show that increasing the spacing promotes a shift toward more stable and synchronous regimes. However, there is no indication of a systematic relationship between regime and spacing (Tables 4, 5, 6) and, unlike Ruzicka et al. (1999, 2000) and Xie and Tan (2003), we did not observe a significant increase in degree of bubbling synchronicity for more widely spaced orifices. We note that fully synchronous bubbling is rare in our experiments (Table 4–6) and it is likely that hydrodynamic interactions among the orifices are responsible for introducing perturbations that suppress synchronization.

Similarly to the single-orifice configuration, the transitions between bubbling regimes do not appear to be sensitive to Capacitance number but are strongly controlled by Weber number (Fig. 12). For a given gas flow rate, Weber number depends on orifice diameter and on the number of orifices and, in the Partly-synchronous, Alternate, and Asynchronous regimes (i.e. the unsynchronized regimes), Weber number will vary from orifice to orifice (values shown in Fig. 12 use mean gas velocity computed according to Eq. (4)). Consequently, the boundaries for different bubbling regimes for multi-orifice bubblers are not as sharply defined as for single-orifice bubblers, and it is not possible to identify a unique range for each orifice diameter. As general trend, a smaller orifice diameter favours the more chaotic and unsynchronized regimes for a given gas flux, with bubbles forming at a higher number of active orifices. A larger orifice diameter favours synchronous behaviour, and fewer orifices are active. Based on the association between Weber number and bubbling regime, we infer that surface tension effects again play an important role. At low Weber number (small orifice diameter or low gas velocity) surface tension dominates, but it is not clear why this is associated with more synchronous behaviour, and with activity at a smaller number of orifices. It is likely that complex resonance between gas pressure in the bubbler and the elastic effects introduced by the surface tension play some role.

5. Conclusions

We performed experiments and identified different bubbling regimes from bubblers with a single orifice, and with multiple in-line orifices in a stagnant liquid. Experimental observations and measurements from high-speed videography allowed us to constrain the processes involved in bubble formation and the effects on bubbling dynamics of varying number and diameter of orifices, bubbler volume, and gas flow rate:

1) For single-orifice bubblers we extend previous experimental studies to higher gas flow rates, and show that published models for bubble volume as a function of gas flow rate are inadequate for regimes in which the wake of a bubble affects the formation of the next bubble.
2) Four different bubbling regimes were identified for in-line multi-orifice bubblers, characterized by varying degree of synchronicity of bubbling among the orifices. Full synchronicity, for the given geometries, orifices configurations and gas flow rates, occurs rarely and only for specific configurations.
3) For decreasing bubbler volumes, bubble period becomes more regular and bubble volume decreases.
4) Both bubble volume and formation time increase for increasing orifice diameter. A larger orifice also favours the development of more stable and synchronous bubbling regimes.
5) Spacing between orifices doesn't play a key role in regime transition.
6) Weber number controls the transition in bubbling regimes for both single-orifice and multi-orifice bubblers.

Based on the experimental data, we built regime maps that allow bubbling behaviour to be predicted from gas flow rate, bubbler volume, and number and diameter of orifices. Our data can also support validation of numerical and CFD models for bubble formation and dynamics in bubblers with multiple in-line orifices.

Acknowledgements

The authors gratefully acknowledge the financial support from the NSFGEO–NERC Grant NE/N018443/1 *Quantifying disequilibrium processes in basaltic volcanism*. The authors also thank Andrew Crosby and Stephen Lishman of the Mechanical Workshop of the Physics Department, Durham University, for their invaluable support in designing and assembling the experimental apparatus, and for laboratory assistance. We thank the journal editor Roberto

Zenit, and two anonymous reviewers for comments that helped improving the manuscript.

References

Acharya, A., Mashelkar, R.A., Ulbrecht, J.J., 1978. Bubble formation in non-Newtonian liquids. Ind. Eng. Chem. Fundam. 17 (3), 230–232.

Badam, V.K., Buwa, V., Durst, F., 2007. Experimental investigations of regimes of bubble formation on submerged orifices under constant flow condition. Canadian J. Chem. Eng. 85 (3), 257–267. doi:10.1002/cjce.5450850301.

Buwa, V.V., Gerlach, D., Durst, F., Schlücker, E, 2007. Numerical simulations of bubble formation on submerged orifices: period-1 and period-2 bubbling regimes. Chem. Eng. Sci. 62 (24), 7119–7132. https://doi.org/10.1016/j.ces.2007.08.061.

Chakraborty, I., Biswas, G., Ghoshdastidar, P.S., 2011. Bubble generation in quiescent and co-flowing liquids. Int. J. Heat Mass Transf. 54 (21-22), 4673–4688.

Chakraborty, I., Biswas, G., Polepalle, S., Ghoshdastidar, P.S., 2015. Bubble formation and dynamics in a quiescent high-density liquid. AIChE J. 61 (11), 3996–4012.

Clift, R., Grace, J.R., Weber, M.E., 1978. Bubbles. Drops and Particles. Academic, New York.

Davidson, J.F., Schuler, B.O.G., 1960a. Bubble formation at an orifice in a viscous liquid. Trans. Inst. Chem. Eng. 38, 144–154.

Davidson, J.F., Schuler, B.O.G., 1960b. Bubble formation at an orifice in an inviscid fluid. Trans. Inst. Chem. Eng. 38, 335–342.

Di Bari, S., Robinson, A.J., 2013. Experimental study of gas injected bubble growth from submerged orifices. Exp. Thermal Fluid Sci. 44, 124–137. https://doi.org/10.1016/j.expthermflusci.2012.06.005.

Gaddis, E.S., Vogelpohl, A., 1986. Bubble formation in quiescent liquids under constant flow conditions. Chem. Eng. Sci. 41 (1), 97–105. https://doi.org/10.1016/0009-2509(86)85202-2.

Idogawa, K., 1987. Effect of gas and liquid properties on the behaviour of bubbles in a column under high pressure. Int. Chem. Eng. 27, 93–99.

Jamialahmadi, M., Zehtaban, M.R., Müller-Steinhagen, H., Sarrafi, A., Smith, J.M., 2001. Study of bubble formation under constant flow conditions. Chem. Eng. Res. Des. 79 (5), 523–532. https://doi.org/10.1205/02638760152424299.

Kulkarni, A.A., Joshi, J.B., 2005. Bubble formation and bubble rise velocity in gas–liquid systems: a review. Ind. Eng. Chem. Res. 44 (16), 5873–5931. doi:10.1021/ie049131p.

Kumar, R., Kuloor, N.K., 1970. The formation of bubbles and drops. In: Advances in Chemical Engineering, 8. Academic Press, pp. 255–368. https://doi.org/10.1016/S0065-2377(08)60186-6.

Leibson, I., Holcomb, E.G., Cacoso, A.G., Jacmic, J.J., 1956. Rate of flow and mechanics of bubble formation from single submerged orifices. II. Mechanics of bubble formation. AIChE J. 2 (3), 300–306. https://doi.org/10.1002/aic.690020306.

Muller, R.L., Prince, R.G.H., 1972. Regimes of bubbling and jetting from submerged orifices. Chem. Eng. Sci. 27 (8), 1583–1592. https://doi.org/10.1016/0009-2509(72)80051-4.

Nahra, H.K., Kamotani, Y., 2003. Prediction of bubble diameter at detachment from a wall orifice in liquid cross-flow under reduced and normal gravity conditions. Chem. Eng. Sci. 58 (1), 55–69. https://doi.org/10.1016/S0009-2509(02)00516-X.

Ruzicka, M., Drahoš, J., Zahradnık, J., Thomas, N.H., 1999. Natural modes of multi-orifice bubbling from a common plenum. Chem. Eng. Sci. 54 (21), 5223–5229. https://doi.org/10.1016/S0009-2509(99)00243-2.

Ruzicka, M., Drahoš, J., Zahradnık, J., Thomas, N.H., 2000. Structure of gas pressure signal at two-orifice bubbling from a common plenum. Chem. Eng. Sci. 55 (2), 421–429. https://doi.org/10.1016/S0009-2509(99)00337-1.

Satyanarayan, A., Kumar, R., Kuloor, N.R., 1969. Studies in bubble formation—II bubble formation under constant pressure conditions. Chem. Eng. Sci. 24 (4), 749–761. https://doi.org/10.1016/0009-2509(69)80066-7.

Schindelin, J., Arganda-Carreras, I., Frise, E., Kaynig, V., Longair, M., Pietzsch, T., Preibisch, S., Rueden, C., Saalfeld, S., Schmid, B., Tinevez, J.Y., 2012. Fiji: an open-source platform for biological-image analysis. Nat. Method 9 (7), 676. doi:10.1038/nmeth.2019.

Sevilla, A., Gordillo, J., Martínez-Bazán, C., 2005. Bubble formation in a coflowing air–water stream. J. Fluid Mech. 530, 181–195. doi:10.1017/S002211200500354X.

Tsuge, H., Hibino, S.I., 1983. Bubble formation from an orifice submerged in liquids. Chem. Eng. Commun. 22 (1-2), 63–79. https://doi.org/10.1080/00986448308940046.

Tsuge, H., Terasaka, K., Koshida, W., Matsue, H., 1997. Bubble formation at submerged nozzles for small gas flow rate under low gravity. Chem. Eng. Sci. 52 (20), 3415–3420. https://doi.org/10.1016/S0009-2509(97)00159-0.

Wang, H., Dong, F., Song, L., 2017. Bubble-forming regime identification based on image textural features and the MCWA feature selection method. IEEE Access 5, 15820–15830. doi:10.1109/ACCESS.2017.2716783.

Xie, S., Tan, R.B., 2003. Bubble formation at multiple orifices—bubbling synchronicity and frequency. Chem. Eng. Sci. 58 (20), 4639–4647. https://doi.org/10.1016/j.ces.2003.06.002.